# Structure and Growth Behavior of Centimeter-Sized Helical Oleate Assemblies Formed with Assistance of Medium-Length Carboxylic Acids†

Yoshiyuki Kageyama,[*,a,b] Tomonori Ikegami,[a] Natsuko Hiramatsu,[a] Sadamu Takeda,[*,a] and Tadashi Sugawara[c]

The nonequilibrium organization of self-assemblies from small building-block molecules offers an attractive and essential means to develop advanced functional materials and to understand the intrinsic nature of life systems. Fatty acids are well-known amphiphiles that form self-assemblies of several shapes. Here, we found that the lengths of helical structures of oleic acid formed in a buffered aqueous solution are dramatically different by the presence or absence of certain amphiphilic carboxylic acids. For example, under the coexistence of a small amount of N-decanoyl-L-alanine, we observed the formation of over 1-centimeter-long helical assemblies of oleate with a regular pitch and radius, whereas mainly less than 100 μm-long helices formed without this additive. Such long helical assemblies are unique in terms of their highly dimensional helical structure and growth dynamics. Results from the real-time observation of self-assembly formation, site-selective small-angle X-ray scattering, high-performance liquid chromatography analysis, and pH titration experiments suggested that the coexisting carboxylates assist in elongation by supplying oleate molecules to a scaffold for oleate helical assembly.

## Introduction

There is increasing interest in the use of highly organized self-assemblies of small building-block molecules for the development of advanced functional materials.[1-3] Research has focused on the spatiotemporal behavior of molecular assembly and, especially, the dynamics of these materials when utilized in life systems[4,5] and soft devices.[6,7] Various experimental and theoretical studies on assembly behavior have been reported and reviewed.[8-10]

Fatty acids are well-known amphiphilic building blocks that can form soft self-assemblies of several shapes, depending on the pH value of the aqueous solution.[11,12] The apparent p$K_a$ (p$K_a^{app}$) values of self-assembled fatty acids differ from the p$K_a$ values of carboxylic acid groups of water-soluble aliphatic acids (e.g., propionic, butyric, and hexanoic acid; Figure 1), which are generally around 4.8.[13] For example, Shah *et al.* reported that the p$K_a^{app}$ of decanoic acid (capric acid) was 7.1–7.3(ref.14) and the p$K_a^{app}$ of oleic acid was 9.85.[15] Therefore, in alkaline aqueous solutions (pH 7–10), fatty-acid assemblies are composed of two types of amphiphiles: a neutral carboxylic acid form and a carboxylate anion form.[16-19] The higher p$K_a^{app}$ values of assembled fatty acids are due to the interaction between carboxylates[14,15,17] and the characteristic dielectric properties and proton activities around the self-assembly surface.[17] These properties change temporally during the nonequilibrium self-assembly process; thus, the acid dissociation of fatty acids fluctuates greatly. For instance, Sugawara *et al.* reported

that several 10 micrometer-sized helical assemblies of oleates in aqueous solution showed spontaneous winding-rewinding motions during helical structure formation, probably owing to fluctuation of the ratio of neutral oleic acid to oleate anion in the assembly.[20]

In the present study, we found that 10 millimeter-sized helical assemblies were formed in an aqueous dispersion of sodium oleate (**ONa**) with 0.1% (w/w) of *N*-decanoyl-L-alanine (**1**) [21-23] (Figure 1), whereas in the absence of **1**, the helical assemblies were less than 300 μm. It is quite rare for such long and well-ordered helical lyotropic assemblies to be formed by the noncovalent assembly of small molecules, such as fatty acids. To elucidate the reason for this elongation of helical assemblies by the additional acid, we investigated the effect of increasing the chain length of the additional aliphatic acids on the elongation of helical assemblies. Here, we describe the observed elongation behavior of helical assemblies derived from the addition of several aliphatic acids, and the structure of helical assemblies according to small-angle X-ray scattering (SAXS). We also propose a possible mechanism for the aliphatic acid-mediated growth of long oleate assemblies, on the basis of the results of growth dynamics observations, pH titration experiments, and high-performance liquid chromatography (HPLC) analysis of the composition of helical assemblies.

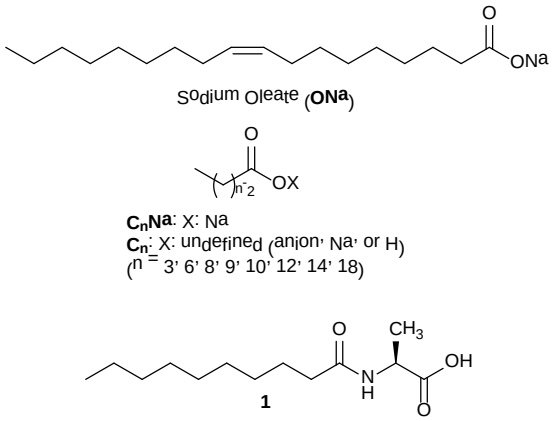


**Figure 1.** Structures of the compounds used in this study.

## Experimental

### General

For microscopic observation, differential interference contrast microscopy (Nikon TE2000 and Olympus IX71S1F) was used. Movies were recorded using USB-CCD cameras (Sentech STC-TC152USB and TOSHIBA JK-TU52H). Movie files were edited and compacted using the Sony Vegas Movie Studio Platinum 9.0 and the Microsoft Movie Maker software packages. An automatic volumetric titrator (Metrohm 877 Titrino Plus) equipped with a pH combination electrode (Lutron PE-11) was used for potentiometric pH titration. Except for the titration experiments, a pH/mV meter (SK-Sato SK-620PH) with the same pH combination electrode was used to determine the pH values of solutions. All pH values were determined by using a standard curve of the measured voltages, obtained with three pH standard solutions (pH 4.01, 6.86, and 10.01). For HPLC analysis, a JASCO LC2000 system, equipped with an Agilent 1260 evaporating light scattering (ELS) detector and an octylsilica reversed

phase column (GL-Science C8-3), was used. $^1$H-NMR spectra of solutions were recorded on a JEOL JEX 270 spectrometer, with tetramethylsilane as an internal reference.

**Materials**

Extra-pure-grade **ONa** was purchased from Junsei Chemical Co., Ltd. and used without further purification. To prove the reliability of observed phenomena, similar experiments were performed while using reagents with different purities purchased from Nacalai Tesque Inc. and Tokyo Chemical Industry Co., Ltd. The formation and elongation of helical assemblies were observed by using reagents purchased from different suppliers. All reagents and distilled water were purchased and used without purification.

**Preparation of *N*-decanoyl-L-alanine (1)[21-23]**

To a mixture of L-alanine (891 mg, 10 mmol) and NaOH (400 mg, 10 mmol) in water (10 mL), 3.5 mL (17.2 mmol) of decanoyl chloride and 14 mL of 1 M NaOH(aq) were added alternately using pipet at 0 °C. After stirring for 1 h at 0 °C and for 1 h at room temperature, 15 mL of 2 M HCl(aq) were added with vigorous stirring. The colorless wet residue obtained after filtration was dissolved in $CH_2Cl_2$. The solution was dried over $Na_2SO_4$, and the solvent was removed under reduced pressure to obtain 3.76 g of crude material. The purified material (colorless crystals, 554 mg, 23% yield) was obtained by recrystallization twice from 10:1 AcOEt: EtOH. $^1$H-NMR δ($CDCl_3$, 270 MHz): 0.88 (t, *J* = 6.3 Hz, 3H), 1.14–1.38 (m, 12H), 1.47 (d, *J* = 7.3 Hz, 3H), 1.58–1.70 (m, 2H), 2.24 (t, *J* = 7.6 Hz, 2H), 4.52–4.64 (m, 1H), 5.99 (br, 1H).

**General method for the formation of helical assemblies and observation of their growth**

A 2:1 chloroform: methanol solution (0.5 mL) containing **ONa** (4.0 mg/mL) and **1** (0.04 mg/mL) was poured into a glass vial. The solvent was evaporated to form a mixed thin film of **ONa** and **1**. One milliliter of bicine-buffered solution (70 mM, pH 7.8) or phosphate-buffered saline (PBS; 75 mM, pH 7.6) was added to the film. The substrates were dispersed by ultrasonication. The dispersion was placed on a glass slide and sealed by a frame-seal (17 × 28 mm) incubation chamber (Bio-Rad). After incubation at 25 °C for 2 h to 7 days, the sample was observed under a microscope. Assemblies with or without other aliphatic acids were observed in a similar manner by using PBS, the pH of which was adjusted between 7.4 and 7.6 to form helical assemblies.

**Compositional analysis of helical assemblies by HPLC**

A dispersion of oleate self-assemblies was prepared by mixing **ONa** (2.4 mg, 7.9 μmol) and **1** (0.031 mg, 0.13 μmol) in 1.2 mL of PBS and incubating the mixture for 10 days at 25 °C. Large assemblies were obtained from the dispersion by absorbing the aqueous phase that included small assemblies, such as micelles and vesicles, with a filter paper. The residue of the large assemblies was dissolved in MeOH and analyzed by HPLC with an ELS detector and an eluent of MeOH: 0.05% TFA(aq) of 78:22. The temperature of the nebulizer was 40 °C , the evaporator was kept at 60 °C, and the flow rate of $N_2$ gas was 1.00 standard liter per minute. For the reference of the HPLC experiments, a MeOH solution of **ONa** and **1**, and the aqueous phase of the dispersion were measured by using the same analysis method. Additionally, the decrease of oleate concentration in the aqueous phase obtained by filtration of dispersion using a 450 nm filter was determined by the same HPLC system with an eluent of MeOH: 0.05% TFA(aq) of 90:10.

**General method for potentiometric pH titration**

Concentration of titrant, 0.5 M HCl solution, was measured using a $Na_2CO_3$ standard solution as a reference. Clear dispersions of a mixture of **ONa** (120 mg, 394 μmol) and additional aliphatic acid sodium salt (39.4 μmol) in 0.1 M NaCl(aq) (60 mL) were prepared in test tubes by ultrasonication. Samples were incubated at 25 °C for approximately 10 min in a water incubation bath, and the titrant was added slowly (by 10-μL stepwise additions) to the test tubes under continuous vigorous stirring to obtain the points on the titration curves.

**Observation of the shape of oleate assemblies in solutions between pH 9.4 and 6.8**

Clear dispersions of **ONa** (118 mg, 389 μmol) in 0.1 M NaCl(aq) (60 mL) were prepared in test tubes by ultrasonication. Each sample was incubated at 25 °C for 10 min in a water bath, and titrant HCl(aq) was added slowly to the test tube using a potentiometric volumetric titrator. At several pH values between pH 9.4 and 6.8 during titration, a small amount of the dispersion was transferred to a slide glass. The sample was subsequently sealed, incubated for 9 h at 25 °C, and observed under a microscope.

**SAXS using synchrotron microbeam X-ray radiation**

SAXS measurements for individual assemblies were carried out at the BL-4A at PF-KEK in Japan.[24] The incident beam was monochromated with a multilayer mirror to be 10 keV and focused to smaller than 5 μm × 5 μm by Kirkpatrick–Baez mirrors. To control the focus and the area of the X-ray beam, an optical microscope system was used. The aqueous sample was placed on a thin glass slide (Matsunami NEO Cover Glass No. 00; thickness: 0.06–0.08 mm) and sealed by a frame-seal incubation chamber. Two-dimensional (2D) images of SAXS patterns were recorded with a 1024 × 1024-pixel IICCD camera (Hamamatsu). To calculate the *d*-spacing from the 2D images, silver behenate diffraction peaks were used as an external reference.[25]

## Results

**Growth of oleate assemblies by the addition of 1**

Mixtures of oleic acid and oleate in an aqueous dispersion self-organize into assemblies of several shapes in a pH-dependent manner.[11,16,20,26] There are two methods for constructing macroscopic tubular, cylindrical, or helical assemblies of oleates. One method is similar to that used in the formation of myelin figures of phosphatidylcholine.[27-32] Namely, an **ONa** paste is hydrated by contact with aqueous buffered solution to grow tubular assemblies from the interface between the paste and the aqueous solution. We previously described another method,[20,33] in which **ONa** is dispersed in an aqueous buffered solution by ultrasonication. Then, the dispersed colloidal oleates gather together to form macroscopic tubular, cylindrical, or helical assemblies, with micelles and vesicles in the bulk solution. In this report, we prepared helical assemblies by the latter method and observed them by differential interference contrast microscopy.

The oleate helical assemblies that were formed without **1** after incubation for 2 days had lengths between 10 and 300 μm, with most assemblies being shorter than 100 μm. When the oleate helical assemblies were formed with 1% (w/w) **1**, millimeter-length helical assemblies were observed after a 2-h incubation.[34] These assemblies showed winding dynamics, and one of their edge was linked to aggregates named the “terminal scaffold” (Figure 2). After incubation for 1 day, we observed over 0.5 centimer-long helical assemblies showing a winding motion (Figure S1 in the Electronic Supplementary Information [ESI]). Similar assemblies of greater than 1 cm in length were observed with the addition of 0.1% (w/w) **1**,

in both bicine-buffered solution (70 mM, pH 7.8; Figure S2 in the ESI) and PBS (75 mM, pH 7.4–7.5). More than 10 helical assemblies of millimeter length were observed in a 120-μL chamber. Assembly shapes included helical assemblies (length = 10–1000 μm), giant vesicles (radius < 100 μm), and block-style aggregates[33] (radius < 10 μm).

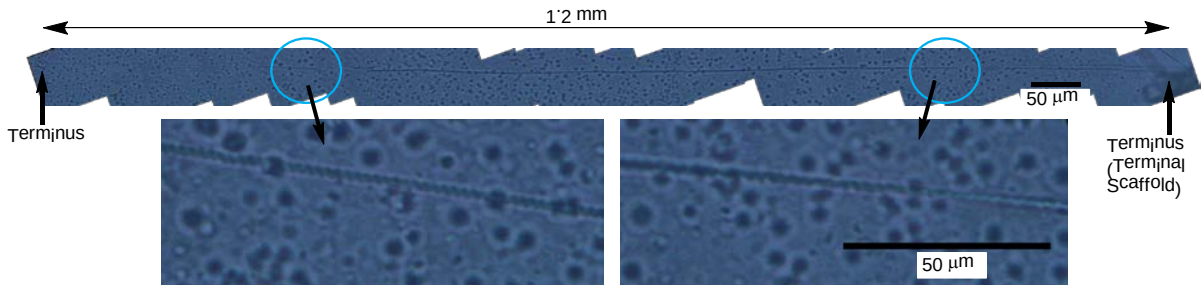


**Figure 2.** Millimeter-length helical assembly composed of oleate formed in the presence of **1** (1% (w/w)) in 70 mM bicine-buffered solution, observed after incubation for 2 h. To show the long-length assembly, figures captured from a movie file were arranged. The lower two images are zoomed-in pictures that clearly show the helical structure. Because of the winding motion of the helical assembly and the Brownian motion of colloidal assemblies, several parts of the assemblies seem to have ruptured.


**Figure 3.** Helical assemblies of oleates formed in the presence of fatty acids. (a) ~2 millimeter-long assembly in the presence of sodium pelargonate (**$C_9$Na**, 1% (w/w)). (b) ~3 millimeter-long assembly in the presence of sodium caprate (**$C_{10}$Na**, 1% (w/w)). Bars indicate 0.1 mm.

### Composition of large oleate assemblies grown in the presence of 1 and change of oleate concentration in the aqueous phase

Through HPLC analysis with an ELS detector, the compositions of the large assemblies, including the helical assemblies and terminal scaffolds, were determined. For large assemblies prepared from **ONa** in the presence of 1.3% (w/w) **1**, only the oleic acid and impurities of the purchased sodium oleate were detected; the amount of **1** was below the lower detection limit of the ELS detector (Figure S3a-c in the ESI). This result indicates that the ratio of **1** in the large assemblies was less than 0.1% (w/w) for **ONa**. It was also revealed that the oleate concentration in the supernatant was quickly decreased by the presence of **1** (Figure S3d in the ESI).

### Growth of oleate assemblies by the addition of various aliphatic acids

Although alanine derivative **1** turns out to be an excellent additive for the elongation of helical assemblies, we are interested in fatty acids as a simpler additive for the same purpose. Several aliphatic

acid sodium salts, including propionate (**$C_3$Na**), caproate (**$C_6$Na**), caprylate (**$C_8$Na**), pelargonate (**$C_9$Na**), caprate (**$C_{10}$Na**), laurate (**$C_{12}$Na**), myristate (**$C_{14}$Na**), and stearate (**$C_{18}$Na**), were mixed with **ONa** and dispersed in PBS (75 mM, pH 7.5) to form helical assemblies. Substantial elongation was observed only in the presence of **$C_9$Na** or **$C_{10}$Na**, and moderate elongation longer than 300 μm was observed in the presence of **$C_8$Na** or **$C_{12}$Na** (Figure S4). In the presence of **$C_9$Na** and **$C_{10}$Na** (1% (w/w)), helical assemblies of several millimeters in length formed (Figure 3). These results indicate that the chain length of the aliphatic acid is a key to the elongation of the helical assemblies of oleates. The specificity of middle-length fatty acid is also found in pH titration experiments.

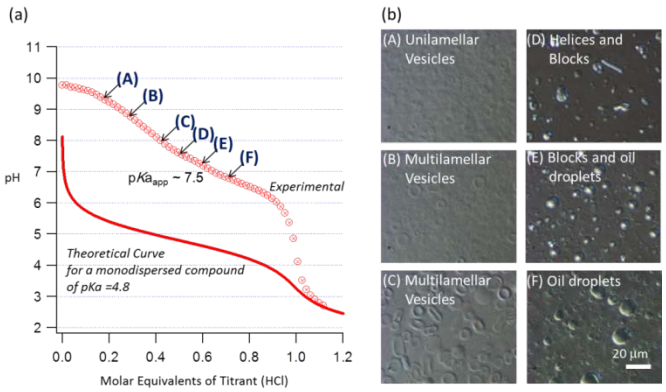


**Figure 4.** (a) Titration curve of 6.6 mM **ONa** in 0.1 M NaCl(aq), with 0.5 M HCl(aq) as the titrant (circles). The line shows the curve calculated by the Henderson–Hasselbalch equation for the sodium salt of a water-soluble acid (p$K_a$ = 4.8), considering the experimental conditions, including ionic strength. (b) Micrographs of assemblies collected at the pH values in (a).

## The pH titration curves of oleate assemblies

Potentiometric pH titration is a fundamental method for estimating or characterizing molecular and colloidal aggregation.[11,14-16,19,35] Cistola *et al.* reported the equilibrium titration curves for potassium oleate at 6 and 40 °C, and discussed the pH-dependent phase behavior of oleates.[11] Their titration curves showed different p$K_a^{app}$ values from those reported by Shah, likely because of the use of different conditions.[15] We determined the pH titration curve for 6.6 mM **ONa**, using 0.5 M HCl(aq) as the titrant in 0.1 M NaCl(aq) at 25 °C. The p$K_a^{app}$ value was approximately 7.5 (Figure 4). The slope of the curve in Figure 4 was related to the macroscopic structure of the oleate assemblies. Helical assemblies were found when the ratio of oleate to oleic acid was approximately 1:1, consistent with the value estimated previously (ca. 3:2) by $^{13}$C-NMR.[20]

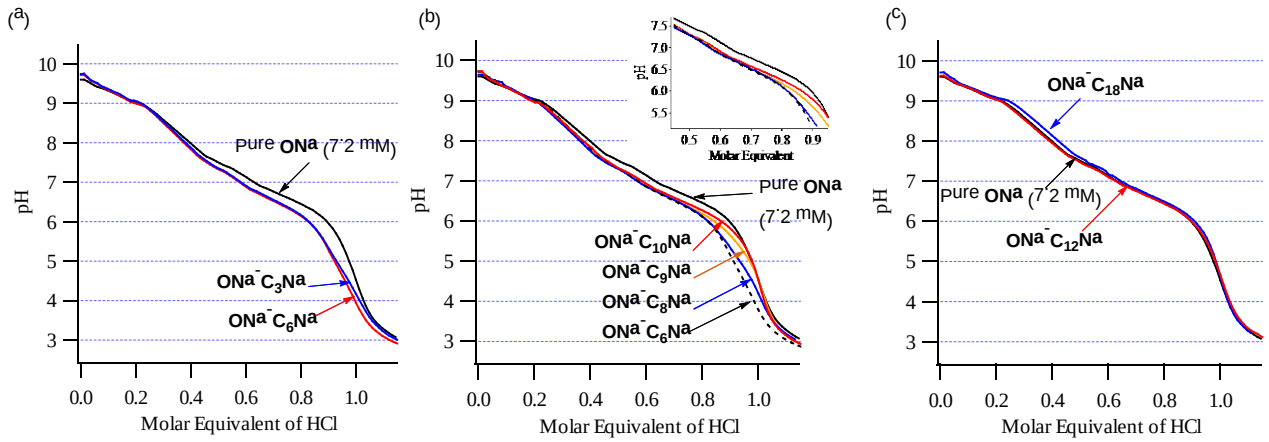


**Figure 5.** Titration curves of 7.2 mM **ONa** (black line in each graph) and mixtures of 6.6 mM **ONa** and 0.66 mM aliphatic acid sodium salts (a) with short-chain carboxylates: **$C_3$Na** (blue) and **$C_6$Na** (red); (b) with medium-chain carboxylates: **$C_6$Na** (dashed), **$C_8$Na** (blue), **$C_9$Na** (orange), and **$C_{10}$Na** (red); and (c) with long-chain carboxylates: **$C_{12}$Na** (red) and **$C_{18}$Na** (blue). The titration curves in (b) are zoomed in the insert.

Titration results for the mixture of **ONa** and 10 mol% aliphatic acid sodium salts (e.g. 3.1% (w/w) **$C_3$Na** and 9.1% (w/w) **$C_{18}$Na**) are shown in Figure 5.[36] Titration curves of the mixture of **ONa** and 10 mol% **$C_{12}$Na** or **$C_{18}$Na** were similar to the curve of **ONa** (Figure 5c). This result indicates that as the titrant was added, the protonation of the long-chain carboxylates occurred concurrently with the protonation of oleate. Thus, the thermodynamic properties of carboxylate protonation for oleic acid and long-chain aliphatic acids were unable to be distinguished in the mixed dispersions. On the other hand, short-chain carboxylates were protonated independently of oleate protonation in the mixed dispersion of **ONa** and 10 mol% **$C_3$Na** or **$C_6$Na** (Figure 5a). This result indicates that the short-chain aliphatic acids dissolved in water and did not interact with the oleate assemblies.

Titration curves of **ONa** with 10 mol% medium-chain aliphatic acid sodium salts (**$C_8$Na**, **$C_9$Na**, and **$C_{10}$Na**) are shown in Figure 5b. The curves clearly show the existence of an interaction between the medium-chain aliphatic acid and oleate at pH values less than 7.4 (for **$C_{10}$Na**), 6.8 (for **$C_9$Na**), and 5.8 (for **$C_8$Na**), whereas the medium-chain aliphatic acid dissolved in solution and did not interact with the oleate assemblies at higher pH values. These results suggest that **$C_9$** and **$C_{10}$** carboxylates were able to disperse dynamically in both bulk solution and oleate assemblies around pH 7, and that the **$C_8$** carboxylate was able to disperse similarly around pH 6, although the shorter-length carboxylates localized in solution and the longer-length carboxylates localized in the oleate assemblies.

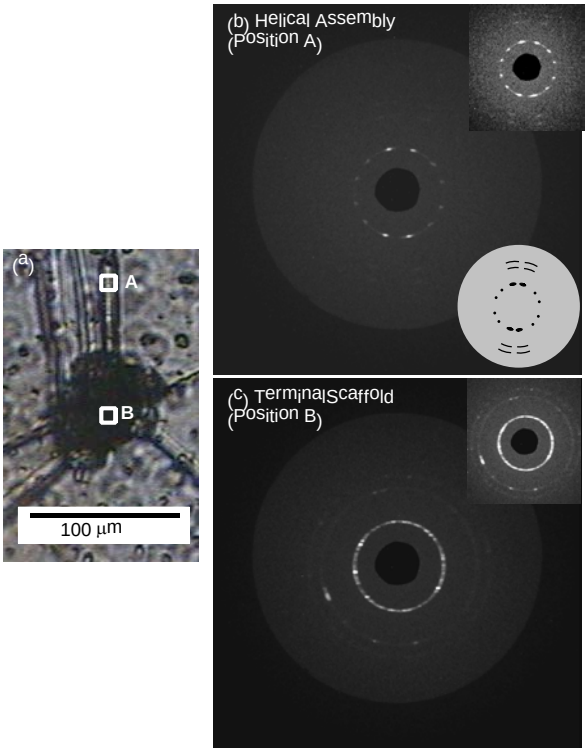


**Figure 6.** Site-selective SAXS for oleate assembly prepared from **ONa** and **$C_9$Na** (1% (w/w)), obtained by synchrotron microbeam X-ray diffraction (KEK PF BL-4A). (a) Optical micrograph of oleate assembly, indicating the two positions (A and B) of analysis. (b) 2D image of the μSAXS pattern collected from the helical assembly at position A in the micrograph. Upper right insert shows the same fringe image with the contrast changed. Lower right insert shows an illustration of the fringe image. (c) SAXS pattern image of the terminal scaffold at location B in the micrograph. The insert shows the same fringe image with the contrast changed.

**Structure of oleate assemblies**

Using the synchrotron microbeam small-angle X-ray scattering (μSAXS) system at BL4A at KEK,[24] we site-specifically measured the microscopic structures of the helical assemblies. Figure 6b shows the fringe image of part of the helical assembly (Figure 6a), which was prepared by dispersing the mixture of **ONa** and 1% (w/w) **$C_9$Na** in PBS (75 mM, pH 7.5). Due to the instability of the assemblies in the presence of the high-brightness X-ray, it was difficult to obtain a highly contrasted fringe image. The diffraction spots were found to lie on three circles (circular arcs) with a Bragg spacing ratio of 1:$\sqrt{3}$:2 (*hk* = 10, 11, and 20), findings that are typical for a hexagonal liquid crystal. The 12 spots on the first ring represented two groups of 6 spots, present every 60 degrees. This finding indicates that there were two hexagonal lattices, both of which belonged to one helical tube (the front and back sides of one helix). The *d*-spacing (5.47 ± 0.08 nm) was calculated by using silver behenate powder (*d* = 5.838 nm)[25] as a reference. On the basis of the μSAXS data, we assume that the helical assemblies had hierarchical structures constructed by hexagonal bundling of inverted tubular micelles of oleates (Figure 7). These helices are macroscopically similar to myelin figures, but their fringe patterns were different from those of myelin figures. Micrographs and SAXS fringe images of dioleoylphosphatidylcholine (DOPC) myelin figures measured using the same apparatus are shown in Figure S5 in the ESI with a schematic illustration of the structure. The ratio of the radius of the first and second fringe circles is 1:2 (*d* = 6.1 ± 0.1 nm),[37] and the spots are not located in a hexagonal pattern but located in a pattern of rotational symmetry, typical for a multilamellar tubular liquid crystal.

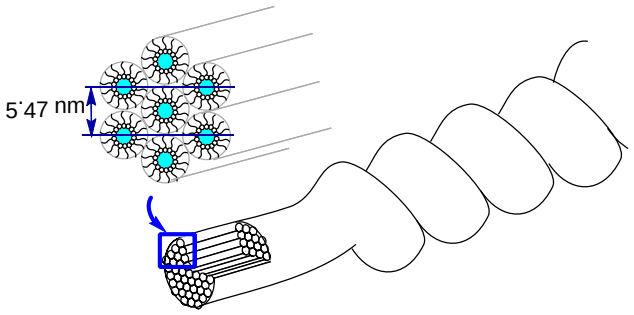


**Figure 7.** Schematic illustration of the oleate helical assembly based on the μSAXS data.

We also measured the terminal scaffold of the helical assembly (Figure 6c). The distributed spots on the circles indicate the macroscopic roughness of the terminal scaffold, but the three circles with a Bragg spacing ratio of 1:√3:2 ($d$ = 5.47 ± 0.08 nm) indicate that the terminal scaffold was in the inverted hexagonal phase.

**Growth dynamics of helical assembly**

We successfully captured a movie of the elongation dynamics of a large-diameter helical assembly in the presence of 0.1% (w/w) **1** at the initial stage of growth (Figure 8 and Movie in the ESI). The helical assembly grew one spire in length with a one-circle winding motion, and this cycle repeated to form a long helical assembly. During elongation of the helical assembly, the size of the terminal scaffold remained almost unchanged. From this evidence, we speculate that oleate molecules dispersed in the bulk solution were continuously supplied to the terminal scaffold during the growth of the long helical assemblies.

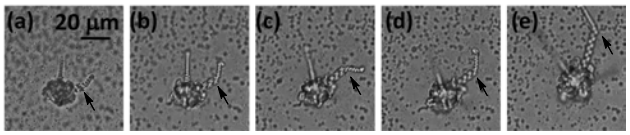


**Figure 8.** Elongation dynamics of a large-diameter helical assembly of oleate in the presence of **1** (0.1% (w/w)). The movie is available in the ESI.

## Discussion

The growth dynamics of molecular assemblies with molecular transport have been of great interest in the fields of material science and nonequilibrium physics for many decades.[38-45] For myelin figures and related assemblies, not only growth dynamics[28,30-32,46-48] but also macroscopic coiling dynamics[29,31,49-53] have been widely studied with experimental and theoretical methods. Although oleate helical assemblies are similar to myelin figures in that they are built from a low-molecular-weight surfactant and have helical macroscopic shapes, our experiments revealed that the inner structure and the observed growth and coiling dynamics of oleate helices are different from those of myelin figures.

In the presence of **1**, millimeter-to-centimeter-scale helical assemblies were formed. Menger and Lee also reported extra-long molecular fibers of several centimeters composed of 5-hexadecyloxy-1,3-benzenedicarboxylate.[54] The detailed structure of the fiber was uncertain, but they assumed that the fiber was constructed by the stacking of disk-like molecular units composed of multiple molecules. On the other hand, we assume that the oleate helical assembly formed in this study had a coiled structure of hexagonally bundled inverted tubular micelles, according to the μSAXS experimental results. Thus, the growth mechanism of the oleate assembly should be different from that of the 5-hexadecyloxy-1,3-benzenedicarboxylate assembly. As Huang *et al*. mentioned,[55] one-dimensional surfactant self-assemblies in solution usually have a length within the nanometer-to-micrometer range. Therefore, we believe that it is important to propose a hypothesis for the growth mechanism of long helical assemblies of oleate.

The oleate helical assemblies were grown from terminal scaffolds, both of which were in the inverted hexagonal phase. The growth was assumed to be a continuous reordering of the kinetically formed preorganized aggregates (terminal scaffolds) to thermodynamically stable ordered structures (helical assemblies). The rate of transformation to a helical assembly in the presence of **1** (0.1% (w/w) or 1% (w/w)) was roughly estimated to be between $10^6$ and $10^8$ molecules per second for each helical assembly, according to real-time observations (Figure S1 and Movie in the ESI). If only transformation proceeds, then the terminal scaffold must become smaller and the helical structure must cease to elongate within a few days (Figure 9a). In fact, helical assemblies prepared from only **ONa** grew several hundred micrometers within one day after dispersion, and they stopped growing due to a shortage of the terminal scaffold. Similarly, the formation of oleate helical assemblies in the presence of **$C_3$Na**, **$C_6$Na**, or **$C_8$Na** (localized in bulk water at pH 7) and **$C_{12}$Na**, **$C_{14}$Na**, or **$C_{18}$Na** (localized in oleate assemblies) also failed to proceed after the terminal scaffolds were consumed.

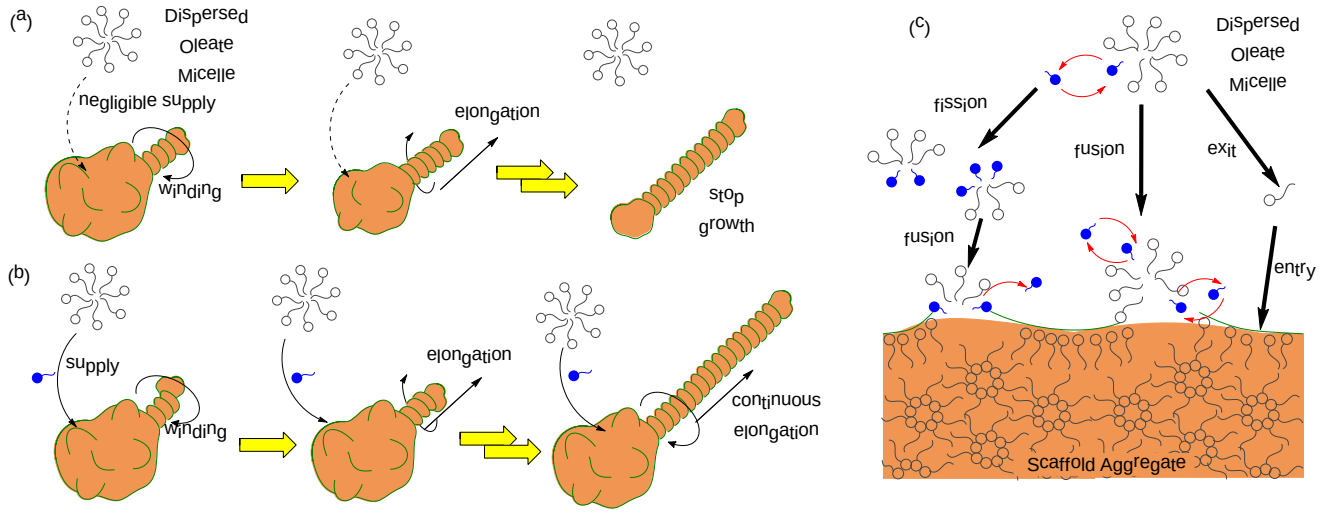


**Figure 9.** Schematic illustration for the elongation of helical assemblies of oleates (a) without and (b) with medium-chain aliphatic acids (indicated by blue color). (c) Three plausible mechanisms, fission-fusion, fusion, and exit-entry, for mediator-assisted molecular supply to the terminal scaffold.

On the other hand, in the presence of **$C_9$Na** or **$C_{10}$Na**, which are phase-transferable between the phases of the oleate assembly and bulk water around pH 7 (Figure 5b), the size of the terminal scaffolds remained unchanged. Therefore, the growth of the helical assemblies continued for a long time. Although it is difficult to assume phase-transfer property of **1** from the pH titration experiment because of its lower p$K_a$ value (Figure S6 in the ESI), this characteristic property of **1** can be realized from two facts. First, the longer hydrophobic chain lengths of **1** than **$C_{10}$** suggest that **1** is favorably adsorbed in the oleate assemblies. Second, the lower p$K_a$ of **1** compared to aliphatic carboxylates suggests that **1** is easy to desorb from oleate assemblies in comparison with **$C_9$** because it should exist in the hydrophilic anion form not only in bulk water but also in the oleate assembly.[56]

Therefore, we propose the following hypothesis for the growth mechanism of long helical assemblies of oleate. During the transformation process of the terminal scaffold into a helical assembly, externally added medium-length aliphatic acids mediate the continuous supply of oleate molecules from the dispersed micelles to the terminal scaffold (Figure 9b). These aliphatic acids make the oleate micelles unstable, transfer oleic acid to the terminal scaffold, and then leave from the terminal scaffold. This hypothesis is supported by their phase-transfer properties, the fact that **1** was not incorporated in the large helical assemblies, and the fact that the decrease of oleate concentration in the aqueous phase was promoted by **1**.

According to the studies on micellar dynamics, three mechanisms are considered for the transport of amphiphiles between self-assemblies: exit-entry, fission-fusion, and fusion (Figure 9c).[40-43] If the supply proceeds via the exit-entry mechanism, then the mediator should act as a surface-active reagent to make the micelles unstable, thus enhancing the dissociation of oleate from the micelles.[57] However, we assume that this mechanism does not operate, because the concentration of monodispersed oleic acid was limited by the critical micelle concentration and, therefore, the kinetics of adsorption to the terminal scaffold were limited. If the supply proceeds via the fission-fusion mechanism, then the mediator acts as a surface-active reagent to stabilize the divided aggregate on the fission process, and decreases the barrier for close contact and adhesion of the divided aggregate to the terminal scaffold on the fusion process. If the supply proceeds via the fusion mechanism, then the mediator decreases the barrier for close contact and adhesion of the micelles to the terminal scaffold. We expect that the mediator molecules promote the fission-fusion or fusion mechanism.[58]

## Conclusions

Helical assemblies of oleate in water are unique because they are well organized, even though the components are assembled by weak noncovalent interactions. From the perspectives of soft-matter physics and supramolecular machine synthesis, helical assemblies are attractive because of their organized macroscopic dynamics. Their spontaneous winding-rewinding dynamics are probably induced by intrinsic fluctuations of the helical assembly,[20] and their rotation-rerotation motions are actuated by photoisomerization of an azobenzene derivative loaded as a minor component in the helical assembly.[33]

Here, we have described the growth dynamics of a centimeter-length helical assembly from a terminal scaffold in the presence of additional carboxylates. To date, only millimeter- and centimeter-length self-assemblies, such as fibers and microtubes composed of amphiphilic molecules, have been

reported.[54,55,59,60] The long helical assembly described here is unique in terms of its hierarchical helical structure and growth dynamics.

We have proposed a possible mechanism for the growth dynamics, in which the small molecules act as mediators to transport building blocks to the terminal scaffold. Although many studies have focused on the nonequilibrium dynamics of molecular assembly, the full mechanism of helical assembly growth has yet to be elucidated. Even if the mediator-assisted elongation of assemblies is a unique phenomenon in the oleate system, the mechanistic aspects of elongation associated with molecular transport can have potential applications in the fields of crystal growth, molecular architecture, and drug delivery systems.

## Acknowledgment

This work was funded by the Sasakawa Scientific Research Grant from the Japan Science Society, JSPS KAKENHI (No. 23750142 and 25620002), and JST PRESTO (Molecular Technology) from MEXT Japan. Microbeam SAXS experiments were performed with approval from the Photon Factory Program Advisory Committee (Proposal No. 2012G747). Y.K. would like to thank Prof. Atsuo Iida (KEK), Dr. Hiroyuki Kitahata (Chiba Univ.), Dr. Mafumi Hishida (Tsukuba Univ.), Dr. Yoshiko Takenaka (AIST), Dr. Yutaka Sumino (Tokyo Univ. of Science), and Dr. Kentaro Suzuki (Kanagawa Univ.) for support on the SAXS measurements, and Dr. Taro Toyota (Univ. Tokyo) for supplying reagents and instruments.

## Notes and references

[a] Department of Chemistry, Faculty of Science, Hokkaido University, Sapporo 060-0810, Japan. E-mail: y.kageyama@mail.sci.hokudai.ac.jp, stakeda@sci.hokudai.ac.jp

[b] JST, PRESTO, Kawaguchi 332-0012, Japan

[c] Department of Chemistry, Faculty of Science, Kanagawa University, Hiratsuka 259-1293, Japan

† Electronic Supplementary Information (ESI) available: The micrographs of centimeter-sized oleate helical assemblies in the presence of a small amount of **1** are shown in Figure S1–S2. Chromatographs for composition analysis are shown in Figure S3. Micrographs of oleate helical assemblies in the presence of several fatty acids are shown in Figure S4. Site-selective SAXS images for DOPC myelin figures and illustration of inner-structure of them are shown in Figure S5. pH Titration curve of mixture of **ONa** and **1** is shown in Figure S6. The growth dynamics of the helical assembly at the initial stage of growth is shown in the Movie. See DOI: 10.1039/b000000x/

1 K. Liu, Y. Kang, Z. Wang and X. Zhang, *Adv. Mater.*, 2013, **25**, 5530-5548.

2 Y. Zhao, F. Sakai, L. Su, Y. Liu, K. Wei, G. Chen and M. Jiang, *Adv. Mater.*, 2013, **25**, 5215-5256.

3 T. Aida, E. W. Meijer and S. I. Stupp, *Science*, 2012, **335**, 813-817.

4 J. M. Zayed, N. Nouvel, U. Rauwald and O. A. Scherman, *Chem. Soc. Rev.*, 2010, **39**, 2806-2816.

5 M. L. Klein and W. Shinoda, *Science*, 2008, **321**, 798-800.

6 N. Giuseppone, *Acc. Chem. Res.*, 2012, **45**, 2178-2188.

7 J. Raeburn, A. Z. Cardoso and D. J. Adams, *Chem. Soc. Rev.*, 2013, **42**, 5143-5156.

8 A. Sorrenti, O. Illa and R. M. Ortuno, *Chem. Soc. Rev.*, 2013, **42**, 8200-8219.

9 M. Ramanathan, L. K. Shrestha, T. Mori, Q. Ji, J. P. Hill and K. Ariga, *Phys. Chem. Chem. Phys.*, 2013, **15**, 10580-10611.

10 F. Li, D. P. Josephson and A. Stein, *Angew. Chem. Int. Ed.*, 2011, **50**, 360-388.

11 D. P. Cistola, J. A. Hamilton, D. Jackson and D. M. Small, *Biochemistry*, 1988, **27**, 1881-1888.

12 As a recent example, C. Hentrich, and J. W. Szostak, *Langmuir*, 2014, **30**, 14916-14925.
13 *CRC Handbook of Chemistry and Physics*, ed. D. R. Lide, CRC Press: Boca Raton, Fl, 82nd edn, 2001.
14 J. R. Kanicky, A. F. Poniatowski, N. R. Mehta and D. O. Shah, *Langmuir*, 2000, **16**, 172-177.
15 J. R. Kanicky and D. O. Shah, *J. Colloid Interface Sci.*, 2002, **256**, 201-207.
16 K. Morigaki and P. Walde, *Curr. Opin. Colloid Interface Sci.*, 2007, **12**, 75-80.
17 S. Salentinig, L. Sagalowicz and O. Glatter, *Langmuir*, 2010, **26**, 11670-11679.
18 F. E. Antunes, L. Coppola, D. Gaudio, I. Nicotera and C. Oliviero, *Colloids Surf. A*, 2007, **297**, 95-104.
19 A. Hirai, H. Kawasaki, S. Tanaka, N. Nemoto, M. Suzuki and H. Maeda, *Colloid Polym. Sci.*, 2006, **284**, 520-528.
20 M. Ishimaru, T. Toyota, K. Takakura, T. Sugawara and Y. Sugawara, *Chem. Lett.*, 2005, **34**, 46-47.
21 A. Pal, Y. K. Ghosh and S. Bhattacharya, *Tetrahedron*, 2007, **63**, 7334-7348.
22 X. H. Luo, B. Liu and Y. Q. Liang, *Chem. Commun.*, 2001, 1556-1557.
23 H. Etori, H. Hirata, Y. Yamada, H. Okabayashi and M. Furusaka, *Colloid Polym. Sci.*, 1997, **275**, 263-273.
24 Y. Nozue, R. Kurita, S. Hirano, N. Kawasaki, S. Ueno, A. Iida, T. Nishi and Y. Amemiya, *Polymer*, 2003, **44**, 6397-6405.
25 T. C. Huang, H. Toraya, T. N. Blanton and Y. Wu, *J. Appl. Cryst.allogr.*, 1993, **26**, 180-184.
26 K. Edwards, M. Silvander and G. Karlsson, *Langmuir*, 1995, **11**, 2429-2434.
27 I. Sakurai, T. Suzuki and S. Sakurai, *Biochim. Biophys. Acta*, 1989, **985**, 101-105.
28 I. Sakurai and Y. Kawamura, *Biochim. Biophys. Acta*, 1984, **777**, 347-351.
29 K. Mishima, K. Fukuda and K. Suzuki, *Biochim. Biophys. Acta*, 1992, **1108**, 115-118.
30 K. Mishima and K. Yoshiyama, *Biochim. Biophys. Acta*, 1987, **904**, 149-153.
31 H. Dave, M. Surve, C. Manohar and J. Bellare, *J. Colloid Interface Sci.*, 2003, **264**, 76-81.
32 L. N. Zou and S. R. Nagel, *Phys. Rev. Lett.*, 2006, **96**, 138301.
33 Y. Kageyama, N. Tanigake, Y. Kurokome, S. Iwaki, S. Takeda, K. Suzuki and T. Sugawara, *Chem. Commun.*, 2013, **49**, 9386-9388.
34 Chiral induction for helical assembly was not observed.
35 As a recent example, G. Charron, D. Huehn, A. Perrier, L. Cordier, C. J. Pickett, T. Nann and W. J. Parak, *Langmuir*, 2012, **28**, 15141-15149.
36 We also performed titration experiments for **ONa** with 1 mol% additional aliphatic acid sodium salt. However, because of the smaller ratio, it was difficult to obtain data in good resolution against the volume of titrant.
37 The *d*-spacing of myelin figure composed of stearoyloleoylphosphatidylcholine was reported as 6.0 nm in G. Paredes-Quijada, H., Aranda-Espinoza, A. Maldonado, *Lipids* **2009**, *44*, 283-289.
38 G. V. Jensen, R. Lund, J. Gummel, M. Monkenbusch, T. Narayanan and J. S. Pedersen, *J. Am. Chem. Soc.*, 2013, **135**, 7214-7222.
39 M. Gradzielski, *Curr. Opin. Colloid Interface Sci.*, 2003, **8**, 337-345.
40 Y. Rharbi and M. A. Winnik, *J. Phys. Chem. B*, 2003, **107**, 1491-1501.
41 Y. Rharbi, M. Karrouch, and P. Richardson, *Langmuir*, 2014, **30**, 797-7952.
42 E. G. Kelley, R. P. Murphy, J. E. Seppala, T. P. Smart, S. D. Hann, M. O. Sullivan and T. H. Epps, *Nat. Commun.*, 2014, **5**, 3599.
43 A. G. Denkova, E. Mendes and M.-O. Coppens, *Soft Matter*, 2010, **6**, 2351-2357.
44 E. A. G. Aniansson, S. N. Wall, M. Almgren, H. Hoffmann, I. Kielmann, W. Ulbricht, R. Zana, J. Lang and C. Tondre, *J. Phys. Chem.*, 1976, **80**, 905-922.
45 E. A. G. Aniansson. and S. N. Wall, *J. Phys. Chem.*, 1974, **78**, 1024-1030.

46 M. Buchanan, S. U. Egelhaaf and M. E. Cates, *Langmuir*, 2000, **16**, 3718-3726.

47 L. Reissig, D. J. Fairhurst, J. Leng, M. E. Cates, A. R. Mount and S. U. Egelhaaf, *Langmuir*, 2010, **26**, 15192-15199.

48 K. Peddireddy, P. Kumar, S. Thutupalli, S. Herminghaus and C. Bahr, *Langmuir*, 2013, **29**, 15682-15688.

49 J. R. Huang, *Eur. Phys. J. E*, 2006, **19**, 399-412.

50 K. C. Lin, R. M. Weis and H. M. McConnell, *Nature*, 1982, **296**, 164-165.

51 I. Tsafrir, M. A. Guedeau-Boudeville, D. Kandel and J. Stavans, *Phys. Rev. E*, 2001, **63**, 031603.

52 V. Frette, I. Tsafrir, M. A. Guedeau-Boudeville, L. Jullien, D. Kandel and J. Stavans, *Phys. Rev. Lett.*, 1999, **83**, 2465-2468.

53 C. D. Santangelo and P. Pincus, *Phys. Rev. E*, 2002, **66**, 061501.

54 F. M. Menger, and S. J. Lee, *J. Am. Chem. Soc.*, 1994, **116**, 5987-5988.

55 Y. Lin, Y. Qiao, X. Cheng, Y. Yan, Z. Li and J. Huang, *J. Colloid. Interface. Sci.*, 2012, **369**, 238-244.

56 To estimate the acid dissociation property that is related to the phase-transfer dynamics, $^{13}$C-NMR measurements in $D_2O$ solution were performed, while using $^{13}$C-enriched *N*-decanoylglycine as a substitute for **1**. However, because of the relatively low p*Ka* of **1** and its substitute, the change of the chemical shift of the enriched carbon was not seen between pH 6 and 9.

57 Related discussions regarding the dynamics of medium-length surfactants have been reported by Vaz's group. Their studies are different from ours in terms of what is transported, but the molecular behaviors may be similar to each other: (a) R. M. S. Cardoso, P. A. T. Martins, F. Gomes, S. Doktorovova, W. L. C. Vaz and M. J. Moreno, *J. Phys. Chem. B*, 2011, **115**, 10098-10108. (b) A. Pokorny, P. F. F. Almeida, E. C. C. Melo, and W. L. C. Vaz, *Biophys. J.* 2000, **78**, 267-280.

58 *N*-Decanoyl-L-alanine (**1**) is a very effective molecule for helix elongation. The precise reason for the high efficiency of **1** is still unknown. Many *N*-acyl amino acids, including **1**, can be reversibly gelated owing to the intermolecular hydrogen bonding between amide groups (ref. 21-23, and a). In addition, it has been proposed that molecular gelation of the inner membrane changes the phase behavior of the membrane to increase its permeability (b and c). These properties may play some roles in the efficient transport of molecules to the terminal scaffold to elongate the helical assembly. (a) A. Ghosh and J. Dey, *Langmuir*, 2009, **25**, 8466-8472. (b) K. J. Skilling, F. Citossi, T. D. Bradshaw, M. Ashford, B. Kellam and M. Marlow, *Soft Matter*, 2014, **10**, 237-256. (c) A. Alex, D. S. Millan, M. Perez, F. Wakenhut and G. A. Whitlock, *Med. Chem. Comm*, 2011, **2**, 669-674.

59 J. Li, N. Huang, D. Wang, L. Xu, Y. Huang, M. Chen, J. Tao, G. Pan, Z. Wu, and L. Li, *Soft Matter*, 2013, **9**, 4642-4647.

60 D. Yan, Y. Zhou and J. Hou, *Science*, 2004, **303**, 65-67.

**Table of Content Figure**

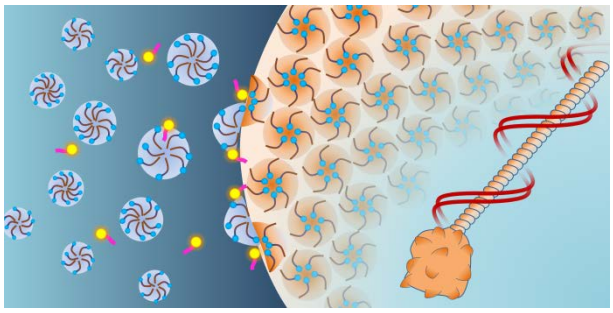

**Back Cover Artwork**